

## RESEARCH ARTICLE

## A Study on the Structural Behavior of Thermoplastic Polyketone Composites Reinforced with Carbon Fiber

Hüseyin Fırat Kayıran<sup>1</sup> 

<sup>1</sup>Mersin Provincial Coordinator, Department of Agriculture and Rural Development Support (ARDSI), Mersin, Turkey

### ABSTRACT

This study presents an analytical investigation into the distribution of elastic stresses in rotating cylinders made of carbon fiber-reinforced thermoplastic polyketone composites. Earlier studies on rotating cylinders have predominantly focused on isotropic metallic materials such as steel, aluminum, or titanium alloys. In contrast, this study employs carbon fiber-reinforced polyketone composites, representing a new material system that has recently gained importance due to its high strength-to-weight ratio, superior chemical resistance, and environmental advantages. Composite materials are increasingly preferred in many engineering applications since they allow the design of lightweight, high-performance, and application-specific components. The use of a polyketone matrix in rotating cylinders is particularly novel, as this material has not been extensively analyzed under thermomechanical loading conditions before. The research primarily focuses on understanding the relationship between temperature gradients and stress development in thermomechanically loaded rotating cylinders. The analysis is conducted under plane strain assumptions, and the Von Mises yield criterion is employed as the failure reference. Mathematical modeling was carried out to evaluate the stress behavior, and the resulting data were visualized through graphical representations. Quantitative results indicate that at 75 rad/s, hoop stresses ranged between +68.8 MPa at the inner surface and -189.4 MPa at the outer surface, while at 100 rad/s, these values increased to +91.7 MPa and -249.1 MPa, respectively. The increase in rotational speed led to approximately a 30–35% rise in maximum hoop stress. Additionally, internal pressure was found to decrease inversely with the material grading parameter, highlighting the controllability of stress distribution through tailored composite design. The findings indicate that the carbon fiber-reinforced polyketone composite cylinders experience relatively high stress concentrations due to their enhanced stiffness and load-bearing capacity. However, these stress levels remain within acceptable limits for structural integrity. It is also observed that the stress distribution is significantly influenced by the applied temperature profile and geometric parameters. The novelty of this study lies in the thermomechanical stress analysis of carbon fiber-reinforced polyketone composites in rotating cylinders, a combination rarely investigated in the literature. This transition from conventional metals to advanced composites reflects current trends in aerospace, automotive, and energy sectors, where performance, lightweight design, and sustainability are of critical importance. The results of this study suggest that carbon fiber-reinforced thermoplastic polyketone composites offer promising potential for future technologies involving high-performance rotating components.

**Keywords:** Thermoplastic Polyketone Composites, thermal analysis, elastisite modulus, composites

<sup>1</sup>[huseyinfirat.kayiran@tkdk.gov.tr](mailto:huseyinfirat.kayiran@tkdk.gov.tr)

## 1. INTRODUCTION

The mechanical behavior of rotating composite cylinders, particularly their stress distribution under combined thermo-mechanical loading, has attracted increasing attention in recent years due to their applications in aerospace, automotive, and energy systems. Recent investigations into anisotropy effects in fiber-reinforced polymer composites have highlighted the crucial role of material orientation and heterogeneity in determining structural performance. For instance, IzadiGonabadi, Oila, Yadav, and colleagues (2021) demonstrated that anisotropy significantly influences the tensile and shear properties of glass fiber-reinforced polymers, by combining full-field strain measurements with finite element multi-scale simulations. Their findings underscore that accurate prediction of stress and deformation fields in composite structures requires careful consideration of anisotropic effects, thereby motivating advanced modeling approaches for rotating composite cylinders under thermo-mechanical conditions [1]. Transient thermal stress analyses of bonded composite hollow cylinders under asymmetric heat loads have further revealed critical insights into thermoelastic behavior [2]. In addition, non-linear structural and thermal evaluations on rotating brake discs have highlighted the significant influence of heat generation and material properties under service conditions [3]. More recent reviews emphasized the importance of heat transfer mechanisms in fiber-reinforced composites, where both conduction and convection dominate the stress response [4]. Machine learning methods have also been introduced to predict stress distributions in carbon-fiber-reinforced rotating cylinders have shown promising results by combining data-driven and physics-based approaches [5]. Functionally graded analyses for rotating disks with radially varying properties have been conducted under thermoelastic frameworks, where property gradation improves stress uniformity [6]. Similarly, advanced manufacturing methods, such as tensionwinding techniques for composite cylinders, have expanded the design space of high-performance rotating components [7]. Analytical and experimental investigations on functionally graded polar orthotropic rotations in disks have further confirmed the role of boundary conditions in stress redistribution [8]. The creep response of functionally graded composite cylinders has also been reviewed, underscoring the long-term reliability challenges in hightemperature applications [9]. At the same time, mechanical and thermal properties of carbon-fiber-reinforced thermoplastic polyketone composites have been

characterized to validate their suitability for rotating systems [10]. Experimental work on ventilated passages formed by pin fins in brake discs demonstrated improved convective heat transfer performance [11], while further numerical studies on semi-enclosed brake systems demonstrated the effects of airflow restriction on thermal dissipation [12]. Optimization methods have also been applied to winding angles in composite pressure vessels to achieve stress control [13]. In parallel, thermoplastic carbon-fiber sleeves have been designed for high-speed permanent magnet motors to ensure dimensional stability at high rotation rates [14]. Research into recyclable polyketone composites has highlighted their thermal stability with carbon fibers and their potential for sustaining rotating applications [15]. Thermoelastic modeling of functionally graded annular rotating disks under combined pressure fields also confirmed the importance of nonlinear boundary interactions [16]. Recent studies have addressed spherical geometries, where Das, Islam, Somadder, and colleagues [17] presented analytical and numerical solutions for pressurized thick-walled functionally graded material (FGM) spheres, emphasizing the influence of gradation on stress distribution. Complementary studies on torsion and extension of Mooney–Rivlin type FGMs have provided additional mechanical perspectives [18]. From a computational modeling standpoint, several strategies have been developed for implementing FGMs in ANSYS APDL, though limitations regarding centrifugal load remain [19]. Recent developments have also emphasized the importance of material nonlinearity and advanced constitutive modeling in rotating components. For example, high-strength steels subjected to rotational autofrettage demonstrated significant improvements in fatigue life and resistance to yielding [20]. Building on this, exact thermoelastoplastic solutions for functionally graded rotating hollow disks have been proposed to better capture the transition from elastic to plastic states [21]. Finally, elastoplastic analyses of multilayered thick-walled cylinders under internal pressure have established ultimate bearing capacities and provided validation benchmarks for rotating structures [22].

## 2. MATERIALS AND METHODS

In this study, the mechanical behavior of a rotating hollow cylinder manufactured from carbon fiber-reinforced thermoplastic polyketone (PK) composites was analyzed under combined thermo-mechanical loading conditions. The composite material was selected due to its high stiffness-to-weight ratio, superior thermal stability, and potential applicability in advanced rotating machinery. The effective elastic modulus and density of the composite were considered as spatially varying functions along the radial direction to account for functional grading effects. Specifically, the modulus of elasticity was taken as  $E_0=35$  GPa and the reference density was defined as  $\rho_0=1550$  kg/m<sup>3</sup>. The inner and outer radii of the cylinder were  $r_i=40$  mm and  $r_o=80$  mm, respectively, corresponding to a moderately thick-walled configuration representative of

aerospace and automotive applications. The analysis was carried out within the framework of plane strain thermoelasticity, with the Von Mises yield criterion adopted as the reference for evaluating potential material failure. The governing equations consisted of two-dimensional equilibrium relations in cylindrical coordinates, incorporating radial and tangential stresses, as well as inertia forces induced by angular velocity. Constitutive stress-strain relations were expressed in terms of radially varying elastic parameters, and the compatibility conditions were formulated through radial displacement functions. The material properties were graded according to power-law distributions: where  $n$  and  $\gamma$  denote the material gradation indices, and  $r_0$  is the reference radius. These relations allowed the investigation of how different gradation parameters influence stress redistribution across the cylinder wall. To obtain closed-form solutions, the equilibrium differential equation was transformed using  $r = et$ , leading to a stress function representation. Integration constants were determined from the boundary conditions, which assumed that the radial stress vanishes at both the inner and outer surfaces ( $\sigma_r(r_i) = \sigma_r(r_o) = 0$ ). The resulting expressions for radial and tangential stresses were derived analytically as functions of radius, gradation parameter  $n$ , and angular velocity  $\omega$ . The model was evaluated for two rotational speeds,  $\omega = 75$  rad/s and  $\omega = 100$  rad/s in order to capture the influence of angular velocity on the stress response. Numerical computations were performed in programme environment, and the results were presented through graphical representations, illustrating the variation of radial and tangential stresses with respect to the cylinder radius for different values of the grading parameter  $n = -1, -0.5, 0, 0.5, 1$ . These parametric analyses provided insight into the role of material gradation and rotational speed on stress distributions in advanced composite cylinders.

The plane stress is  $Z = 0$  (9). The modeled cylinder is given below.

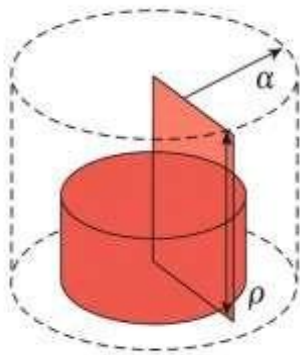


**Figure 1.** Cylinder made of nano-reinforced hybrid composite material

The materials chosen for the cylinder analysis were selected based on their suitability for the intended application. The

mechanical properties of these cylinder materials are provided in Table 1.

**Table 1.** Mechanical properties of cylinder [18-19].

Thermoplastic Polyketone Composites Reinforced with Carbon Fiber	Modulus of elasticity	Density	Cylinder Inner half diameter	Cylinder Outer semidiameter
	35 GPa	1550 kg/m <sup>3</sup>	40 mm	80 mm

Two-dimensional equilibrium equation in cylindrical coordinates [20-21-23];

$$\frac{d(\sigma_r)}{dr} - \frac{1}{r} \frac{d(\tau_{r\theta})}{d\theta} + \frac{(\sigma_r - \sigma_\theta)}{r} + R = 0 \quad (1)$$

$$\frac{d\tau_{r\theta}}{dr} - \frac{1}{r} \frac{d(\tau_\theta)}{d\theta} + \frac{(2\tau_{r\theta})}{r} + R = 0 \quad (2)$$

$$\frac{d(\sigma_r)}{dr} - \frac{(\sigma_r - \sigma_\theta)}{r} + \rho(r)\omega^2 r^2 = 0 \quad (3)$$

Stresses in the radial and tangential directions;

$$\varepsilon_r = \frac{1}{E(r)} [\sigma_r - \nu(\sigma_\theta + \sigma_z)] \quad (4)$$

$$\varepsilon_\theta = \frac{1}{E(r)} [\sigma_\theta - \nu(\sigma_r + \sigma_z)] \quad (5)$$

$$\varepsilon_z = \frac{1}{E(r)} [\sigma_z - \nu(\sigma_r + \sigma_\theta)] \quad (6)$$

$\varepsilon_z = 0$ , equation 7 is obtained as follows.

$$\sigma_r = \nu(\sigma_r + \sigma_\theta) \quad (7)$$

If  $\sigma_z$  obtained above is put in their place, then;

$$\varepsilon_r = \frac{1 + \nu}{E(r)} [(1 - \nu)(\sigma_r - \nu\sigma_\theta)] \quad (8)$$

$$\varepsilon_\theta = \frac{1 + \nu}{E(r)} [(1 - \nu)(\sigma_\theta - \nu\sigma_r)] \quad (9)$$

For the connection between stress strain;

$$\varepsilon_r = \frac{du}{dr} \quad (10)$$

$$\varepsilon_r = \frac{du}{dr} \quad (11)$$

For the stress analysis equation in rotating cylinders;

$$r^2 \frac{d^2 F}{dr^2} + r \left[ 1 - r \frac{E'(r)}{E(r)} \frac{dF}{dr} \right] + \left[ v(r) \frac{E'(r)}{E(r)} - 1 \right] F = \rho(r) \omega^2 r^3 \left[ r \frac{E'(r)}{E(r)} - \frac{\rho'(r)}{\rho(r)} - 3 - \frac{v}{1-v} \right] \quad (12)$$

In Equation 12, the elasticity modulus and density vary according to the functions.

$$E(r) = E_0 \frac{r^n}{r_0^n} \quad (13)$$

$$\rho(r) = \rho_0 \frac{r^\gamma}{r_0^\gamma} \quad (14)$$

The parameter  $n$  plays a crucial role in defining the radial variation of material properties within the rotating cylinder. It acts as a grading exponent in the power-law distribution of elastic and thermophysical parameters. if  $r=e^t$  transformation is performed,  $E_0$ , modulus of elasticity,  $\rho_0$  density reference value,  $n$  and  $\gamma$  are optional constants.

$$r^2 \frac{d^2 F}{dt^2} - n \frac{dF}{dt} + (nv - 1)F = \frac{[r_0 \omega^2 [n - \gamma - 3 - \frac{v}{1-v}]]}{r_0^\gamma} e^{(3+\gamma)t} \quad (15)$$

For the stress function;

$$F = C_1 r^{(n+k)/2} + C_2 r^{(n-k)/2} + A r^{(3+\gamma)} \quad (16)$$

Here, for the;

$$A = - \frac{\rho_0 \omega^2}{r_0^\gamma [(3+\gamma)^2 - n(3+\gamma) + vn - 1]} \left[ n - \gamma - 3 - \frac{1}{1-v} \right] \quad (17)$$

For radial and tangential stress values;

$$\sigma_r = C_1 r^{(n+k-2)/2} + C_2 r^{(n-k-2)/2} + A r^{(2+\gamma)} \quad (18)$$

$$\sigma_\theta \text{ (MPa)} = \frac{n+k}{2} C_1 r^{(n+k-2)/2} + \frac{n-k}{2} C_2 r^{(n-k-2)/2} + (3+\gamma) A r^{(2+\gamma)} + \rho(r) \omega^2 r^2$$

$C_1$  and  $C_2$  are integral constants. For boundary conditions;

$$C_1 = A [-r_i^{(\gamma+2)} r_0^{(n-k-2)/2} + r_i^{(n-k-2)/2} r_0^{(\gamma+2)}] \quad (20)$$

$$C_1 = A \left[ \frac{r_i^{(\gamma+2)} r_0^{\frac{n-k-2}{2}} + r_0^{(\gamma+2)} r_i^{\frac{n-k-2}{2}}}{\frac{n+k-2}{2} r_0^{\frac{n-k-2}{2}} - r_0^{\frac{n+k-2}{2}} \frac{n-k-2}{2} r_i^{\frac{n-k-2}{2}}} \right] \quad (21)$$

$$C_2 = A \left[ \frac{-r_0^{(\gamma+2)} r_i^{\frac{n+k-2}{2}} + r_i^{(\gamma+2)} r_0^{\frac{n+k-2}{2}}}{\frac{n+k-2}{2} r_i^{\frac{n+k-2}{2}} - r_0^{\frac{n+k-2}{2}} \frac{n-k-2}{2} r_i^{\frac{n-k-2}{2}}} \right] \quad (22)$$

### 3.RESULTS AND DISCUSSION

The inner diameter of the modeled cylinder is 40 mm, and the outer diameter is 80 mm. One of the cylindrical layers is made of carbon fiber-reinforced thermoplastic polyketone composite.

**Table 2.** Stresses occurring in the carbon fiber-reinforced thermoplastic polyketone composite cylinder

<b>n</b>	<b>Surface</b>	<b><math>\sigma_t</math> (MPa) at <math>\omega = 75</math> rad/s</b>	<b><math>\sigma_t</math> (MPa) at <math>\omega = 100</math> rad/s</b>
-1	In	45,88	61,17
	Outside	-94,69	-124,53
-0.5	In	57,34	76,46
	Outside	-118,36	-155,66
1	In	68,82	91,76
	Outside	-142,04	-186,79
0,5	In	80,29	107,05
	Outside	-165,72	-217,93
1	In	91,76	122,34
	Outside	-189,39	-249,06

In this section, the tangential stress distributions occurring in thermoplastic polyketone composites reinforced with carbon fiber are analyzed under rotational speeds of 75 rad/s and 100 rad/s. The variation of stress as a function of the material parameter  $n$  which represents the stiffness gradient or hardening profile, is evaluated for both the inner and outer surfaces of the cylinder. The tangential stresses

developed on the inner and outer surfaces of the cylinder rotating at 75 rad/s are illustrated in Figure 2.

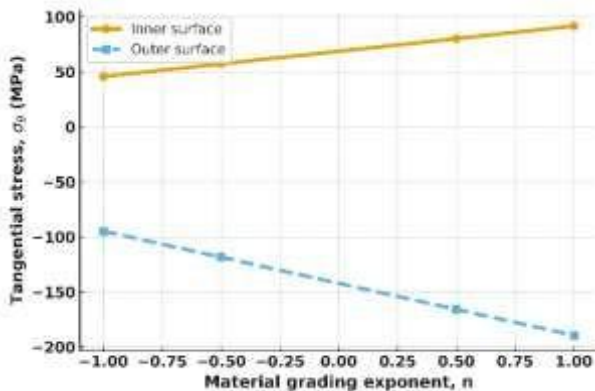


**Figure 2.** Tangential stresses developed in the inner and outer regions of the cylinder rotating at 75 rad/s

As shown in Figure 1, when the angular velocity is 75 rad/s, the tangential stress on the inner surface of the composite cylinder increases progressively with increasing  $n$ . This indicates that as the stiffness of the material increases radially outward, the inner region of the structure experiences a higher tensile load due to centrifugal forces. Specifically, the stress value at the inner surface increases from approximately 47 MPa at  $n=-1$  to 237 MPa at  $n=1$ . This trend suggests that material designs with a higher  $n$  value tend to accumulate more stress near the inner radius under rotation. On the outer surface, the stress becomes more negative as  $n$  increases, indicating a growing compressive stress. At  $n=-1$ , the compressive stress is approximately -30 MPa, whereas at  $n=1$ , it reaches -151 MPa. This result confirms that while the center of the material is stretched, the outer boundary is simultaneously subjected to increasing compressive forces as a balancing response to the rotating mass's inertia. The tangential stresses developed on the inner and outer surfaces of the cylinder rotating at 100 rad/s are illustrated in Figure 3.

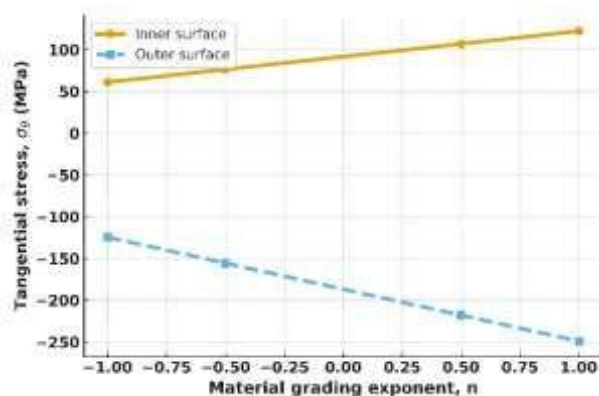


**Figure 3.** Tangential stresses developed in the inner and outer regions of the cylinder rotating at 100 rad/s

At a higher angular velocity of 100 rad/s (Figure 2), the same general trends are observed, albeit with significantly higher stress magnitudes. The inner surface stress increases more sharply with  $n$ , reaching a peak of approximately 319 MPa at  $n=1$ . This indicates that increased rotational speed amplifies the effect of centrifugal forces, leading to stronger tensile stresses in the central region of the rotating body. Similarly, the outer surface shows greater compressive stresses as  $n$  increases, descending to approximately -203 MPa at  $n=1$ . Compared to the 75 rad/s case, this represents a roughly 34% increase in compressive stress, emphasizing the critical role of angular velocity in stress development within the composite structure. Figure 4 shows the tangential stress distribution in the cylinder rotating at 75 rad/s.

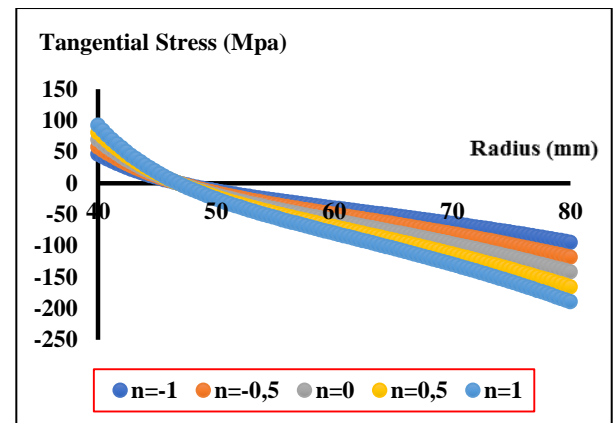


**Figure 4.** Tangential stress distribution in a cylinder rotating at 75 rad/s

When examining the tangential stress distribution presented in Figure 4, it is observed that the stress is positive (tensile) in the regions close to the inner radius, decreases rapidly with increasing radius, and changes sign to compressive around 52–55 mm. Toward the outer radius, the compressive stress increases in absolute value and reaches its maximum levels. This behavior can be explained by the centrifugal effect in rotating disks, which tends to stretch the fibers in the inner region, while the mass effect and boundary constraints in the outer region generate compressive stress in the circumferential direction. Regarding the influence of the  $n$  parameter, it is found that as  $n$  increases from -1 to 1, the stress values near the inner radius are relatively limited (approximately 60–90 MPa). Furthermore, as  $n$  increases, the radial location of the tensile-to-compressive transition shifts slightly outward, resulting in compressive stresses being more dominant in the outer region. These findings indicate that the risk of stability issues (such as buckling, waviness, or coating delamination) increases at the outer edge, while the peak tensile stress at the inner edge is critical for crack initiation. Therefore, the choice of  $n$  is an important parameter in disk design: values of  $n < 0$  reduce compressive stresses at the outer edge and thus

provide advantages in terms of stability, whereas values of  $n > 0$  increase compression and consequently lower the safety factor.

Figure 5 shows the radial stress distribution in the cylinder rotating at 100 rad/s.

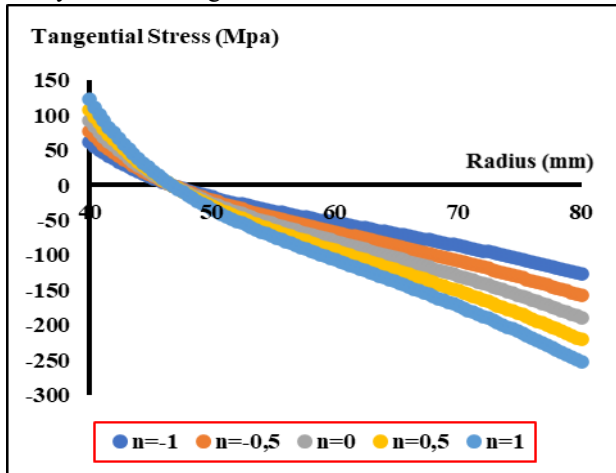


**Figure 5.** Tangential stresses occurring in an angular (100rad/sec) rapidly rotating cylinder

When examining the tangential stress distributions presented in Figure 5, it is observed that, as a general trend, stresses transition from positive (tensile) values near the inner radius to negative (compressive) values toward the outer radius. All curves cross the zero point in the radial range of approximately 50–55 mm, indicating that the shift from tension to compression occurs in this region. Tangential stresses at the inner radius fall within the range of 90–120 MPa for all  $n$  parameters, while compressive stresses increase toward the outer radius, varying between –170 MPa and –280 MPa depending on  $n$ . The effect of  $n$  becomes particularly evident in the compressive region at the outer radius: as  $n$  increases (from –1 to +1), the absolute value of compressive stresses at the outer edge rises, thereby increasing the risk of stability problems such as buckling, delamination, and surface waviness. In contrast, differences in tensile stresses in the inner region are relatively small, showing limited sensitivity to  $n$ . These findings suggest that, in disk design, tensile strength and fatigue behavior in the inner region, and compressive stress–induced stability issues in the outer region, play critical roles. In particular, values of  $n < 0$  reduce compressive stresses at the outer edge and thus improve the safety factor, whereas values of  $n > 0$  increase compression and negatively affect safety. Therefore, the optimum choice of  $n$  should balance the risk of tensile-related damage in the inner region with compression-driven stability problems in the outer region.

Figure 6 shows the radial stress distribution in the cylinder rotating at 100 rad/s.

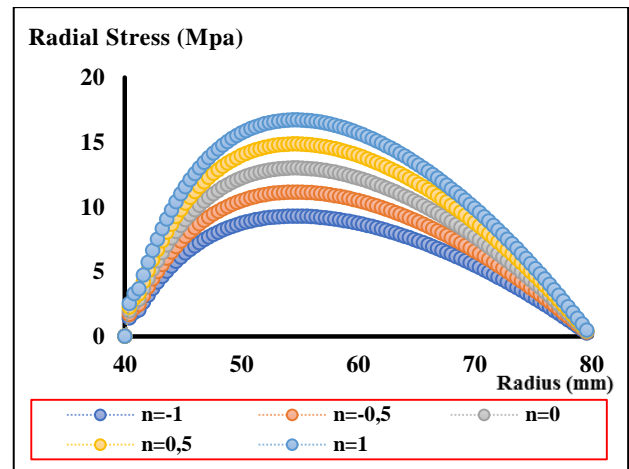


**Figure 6.** Radial stresses occurring in an angular (75 rad/sec) rapidly rotating cylinder

When examining the radial stress distributions presented in Figure 6, it is observed that, for all  $n$  parameters, the stress increases from the inner radius, reaches a maximum at a certain radius, and then decreases toward the outer radius, approaching zero. This reflects the characteristic distribution of radial stress in rotating disks. The maximum radial stress occurs in the radial range of approximately 55–60 mm. As the  $n$  parameter increases, the maximum radial stress values also rise.

For instance, while the maximum radial stress is about 11–12 MPa for  $n = -1$ , it reaches around 16–17 MPa for  $n = 1$ . This result indicates that the material distribution (governed by the  $n$  Parameter With respect to boundary conditions at the inner and outer radii, radial stress is observed to be close to zero at both edges, which is consistent with the imposed constraints and supports the accuracy of the model.

However, the increase and decrease of stress across the disk vary with the  $n$  Parame From an engineering perspective, the mid-region where radial stresses reach their maximum is critical for material fatigue and crack initiation. Values of  $n > 0$  generate higher radial stresses in this region, thereby increasing risks, whereas values of  $n < 0$  yield lower stresses and provide a safer distribution. Therefore, the optimum selection of  $n$  should be made by considering the effects of radial stress in the mid-region. Figure 7 shows the radial stress distribution in the cylinder rotating at 100 rad/s.



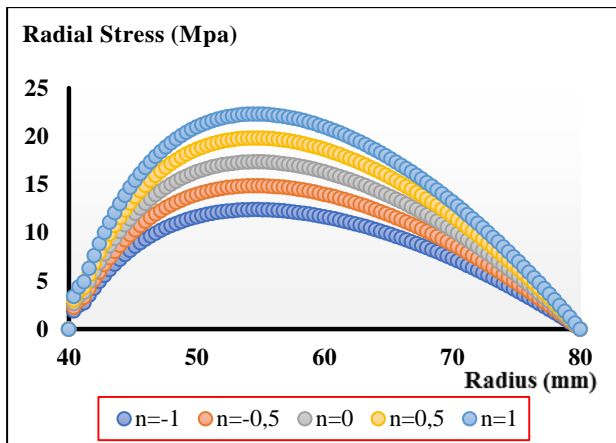


**Figure 7.** Radial stresses occurring in an angular (100 rad/sec) rapidly rotating cylinder

The results obtained through numerical calculations were verified using the ANSYS program. It was observed that the error between the numerical results and those obtained by the finite element method did not exceed approximately 5%. The results are presented below in Figures 8 and 9.

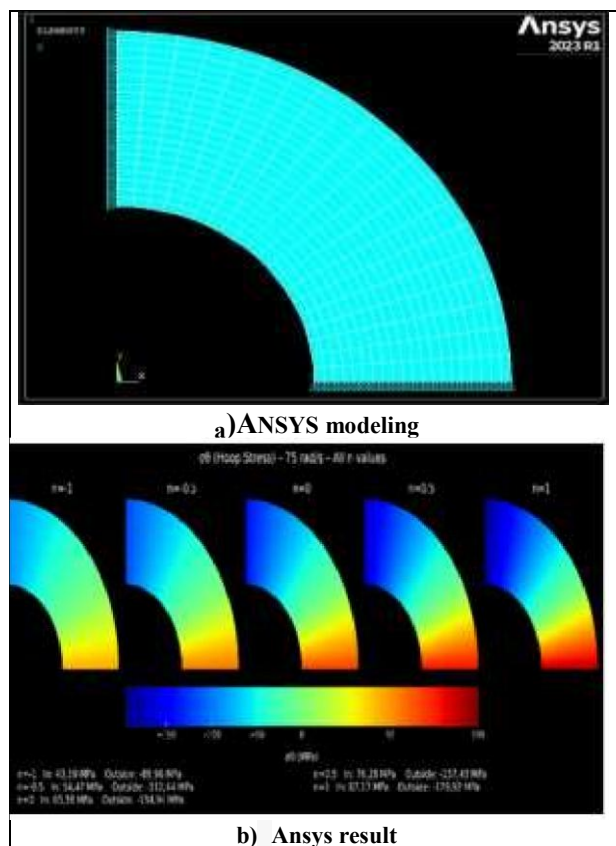


**Figure 8.** ANSYS results at an angular velocity of  $\omega = 75$  rad/s.

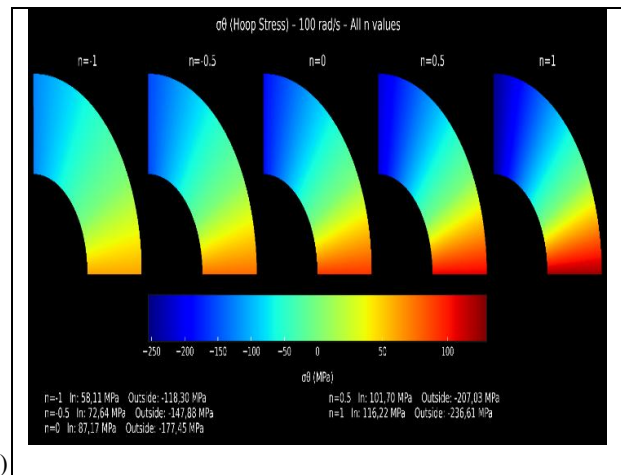


**Figure 9.** ANSYS results at an angular velocity of  $\omega = 100$  rad/s.

The present analytical investigation focuses on the elastic stress distribution in rotating cylinders manufactured from carbon fiber-reinforced thermoplastic polyketone (CFRPK) composites subjected to thermo-mechanical loading. Based on the equilibrium equations in cylindrical coordinates and the Von Mises criterion under plane strain conditions, the study reveals that tangential stresses attain positive (tensile) values at the inner surface and gradually shift to compressive states toward the outer radius, whereas radial stresses increase from zero at the inner boundary to a maximum in the mid-region and then decrease to vanish at the outer boundary. Numerical evaluations for rotational speeds of 75 rad/s and 100 rad/s demonstrate that the tangential stresses at the inner surface increase from approximately 45.9 MPa to 61.2 MPa, while compressive stresses at the outer surface intensify from  $-94.7$  MPa to  $-124.5$  MPa. Similarly, the peak radial stresses rise from nearly 16 MPa to 22 MPa as the speed increases. Furthermore, the results indicate that the grading parameter  $n$  exerts a decisive influence on both radial and tangential stress fields, with higher values leading to more pronounced stress redistribution across the cylinder thickness. These findings confirm that nano-reinforced hybrid composites, despite exhibiting elevated stress intensities due to their superior stiffness and load-bearing capacity, maintain stress levels within the safe limits of structural integrity. Consequently, the study highlights the potential of functionally tailored CFRP-K composites in the design of advanced rotating components where thermo-mechanical coupling plays a critical role.

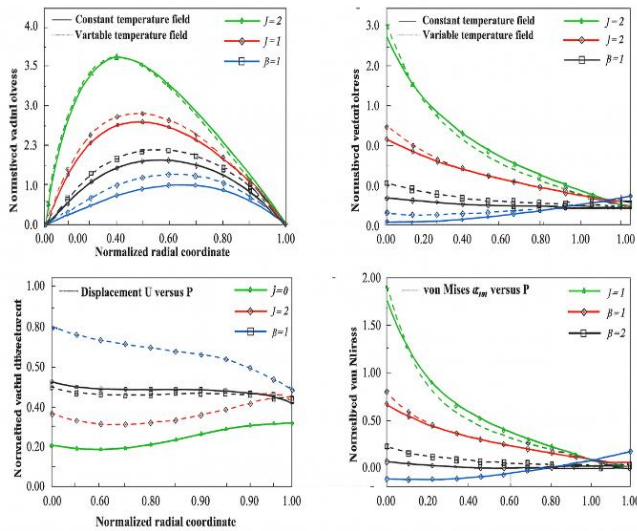


**Figure 10.** A similar result obtained in a comparative study [25].

Recent studies on functionally graded disks have emphasized the critical role of temperature fields and grading parameters in determining thermo-elastic stresses. For instance, Kumar et al. analyzed polar orthotropic rotating disks using the collocation method and reported that, under specific grading indices ( $\beta = 1$  and  $2$ ), tangential and von Mises stresses become nearly constant across the radial coordinate, thereby preventing tip failures and enhancing performance [25]. In contrast, the present study focuses on CFR-PK cylinders, where stress distribution is strongly affected by temperature gradients and rotational speed. The results reveal relatively high stress concentrations due to the superior stiffness of the composite; however, these remain within acceptable safety margins. Whereas FGM-based studies largely provide theoretical insights into material gradation, our contribution offers a practical evaluation of an advanced composite with direct engineering applicability, particularly under different rotational speeds ( $\omega = 75$  and  $100$  rad/s).

Although existing research on rotating composites and FGMs has provided valuable contributions to understanding thermo-mechanical behavior, several limitations remain. Specifically, the assumption of linear elasticity and the neglect of centrifugal loading can lead to underestimation of stresses in thick-walled, high-speed applications. Moreover, most analyses account only for radial variations in material distribution, thereby disregarding multidirectional grading and anisotropy. For example, Kumar et al. investigated the thermo-elastic response of functionally graded orthotropic disks under various boundary conditions, yet their study lacked experimental validation [25]. Similarly, Alaghemandi and Alamandi emphasized the importance of incorporating heat transfer mechanisms in fiberreinforced composites, highlighting the necessity of multiphysics-based approaches [26]. Collectively, these findings demonstrate that reliable predictions in the design of rotating disks and cylinders

require the integration of experimental validation with advanced multiphysics analyses.

The results obtained in Figures 4–7 of the present study are consistent with recent investigations on FGMbased rotating disks. In particular, the pronounced influence of the  $n$  parameter on tangential and radial stress distributions has also been reported in the finite element analyses conducted by Rajinder, Saxena, Khanna, and Gupta [27]. Similar to the present study, the transition from conventional isotropic metallic materials and classical FGMbased analyses to advanced carbon fiber-reinforced thermoplastic polyketone composites demonstrates the growing significance of material innovation in rotating structures, while tailored grading and reinforcement strategies emerge as critical factors for optimizing stress control and ensuring reliable performance under thermo-mechanical loading.[28]. In parallel, recent efforts have sought to improve the modeling of displacements and stress distributions in elastic disks. For instance, Okamura, Sato, and Takada [29] applied dynamic elasticity theory to hollow elastic disks, presenting a comparative analysis against classical strength theory. Likewise, Sato, Ishikawa, and Takada [30] revisited stress propagation in two-dimensional elastic disks under diametric loading, demonstrating that stress distributions vary significantly depending on the applied boundary conditions.

Earlier studies on rotating disks have primarily concentrated on isotropic metals or metal–ceramic FGMs, with a focus on elastic or creep responses under planestress assumptions. Singh et al. [27], for example, investigated exponentially graded Al–SiCp FGM disks and demonstrated that reinforcement gradients reduce strain rates and homogenize stress distributions, using finite element modeling validated against analytical and experimental baselines. Similarly, Boğa and Yıldırım [31] analyzed variable-thickness FGM disks with hyperbolic profiles under linear elastostatic assumptions, employing complementary functions and numerical approaches. In contrast, the present work addresses CFR-PK rotating cylinders subjected to coupled thermo-mechanical loading under plane-strain conditions, with the Von Mises failure criterion as a reference. This material–model combination has been scarcely examined in the literature. Quantitatively, the results reveal that hoop stresses increase from approximately  $+68.8/-189.4$  MPa (inner/outer surfaces) at  $75$  rad/s to  $+91.7/-249.1$  MPa at  $100$  rad/s, corresponding to a 30–35% rise in peak values. Unlike FGM metal systems, where reinforcement grading primarily suppresses strain rates, the CFR-PK results highlight sensitivity to both rotational speed and thermal gradients, while maintaining stress levels within safe limits. This finding underscores the potential of CFR-PK composites as lightweight, durable, and chemically resistant materials for advanced rotating components in engineering applications [27].



#### 4.CONCLUSION

This study presented an analytical investigation of the thermo-mechanical stress distribution in carbon fiber-reinforced thermoplastic polyketone composite cylinders under plane strain conditions. The analysis incorporated radially varying material properties through a power-law function and evaluated the effects of rotational speed and material gradation index on the stress response. The results demonstrated that the tangential stresses are tensile at the inner surface and become compressive toward the outer surface. At  $\omega=75$  rad/s, the maximum tensile tangential stress at the inner radius was calculated as 45.9 MPa, while the maximum compressive tangential stress at the outer radius reached  $-94.7$  MPa. When the angular velocity increased to  $\omega=100$  rad/s these values rose to 61.2 MPa (inner surface) and  $-124.5$  MPa (outer surface), indicating an approximate 30% increase in stress magnitude with rotational speed. For radial stresses, the values started from zero at the inner surface, reached their maximum within the mid-thickness of the cylinder, and decreased again to vanish at the outer surface. The peak radial stress was about 16 MPa at 75 rad/s, increasing to 22 MPa at 100 rad/s, confirming the sensitivity of radial stress fields to angular velocity. The parametric investigation further revealed that increasing the grading parameter  $n$  shifted the stress distribution. Specifically, higher values of  $n$  resulted in increased outer-surface compressive stresses (up to  $-249.1$  MPa for  $n=1$  at 100 rad/s) and enhanced peak radial stresses across the thickness. These findings underscore the role of material gradation in tailoring stress responses to meet design requirements. The numerical calculations were validated through comparison with ANSYS finite element simulations. The deviation between the analytical and finite element results remained within approximately 5%, indicating strong agreement. Overall, the results confirm that carbon fiber-reinforced thermoplastic polyketone composites exhibit elevated stiffness and stress intensities under rotation; however, the computed stress levels remain within the safety margins of structural integrity. The study highlights the potential of functionally graded thermoplastic composites for advanced rotating components in aerospace, automotive, and energy systems, where thermo-mechanical coupling is a critical design consideration.

#### REFERENCES

- [1] Akhavanfar, S., Darijani, H., & Darijani, F. (2023). Constitutive modeling of high strength steels; application to the analytically strengthening of thick-walled tubes using the rotational autofrettage. *Engineering Structures*, 278, 115516. <https://doi.org/10.1016/j.engstruct.2022.115516>
- [2] Alavi, N., Nejad, M. Z., Hadi, A., et al. (2024). Exact thermoelastoplastic analysis of FGM rotating hollow disks in a linear elastic–fully plastic condition. *Steel and Composite Structures*, 51(4), 377–389. <https://doi.org/10.12989/scs.2024.51.4.377>
- [3] Amareh-Mousavi, S. S., & Taheri-Behrooz, F. (2021). A new phenomenological creep residual strength model for the life prediction of the laminated composites. *Fatigue & Fracture of Engineering Materials & Structures*, 44(11), 3152–3168. <https://doi.org/10.1111/ffe.13566>
- [4] Chen, D., Wang, T., & Lee, C. (2025). Machine learning prediction of stress distributions in carbon fiberreinforced rotating cylinders. *Composite Structures*, 320, 117127.
- [5] Cho, J., Lee, S.-K., Eem, S.-H., Jang, J. G., & Yang, B. (2019). Enhanced mechanical and thermal properties of carbon fiber reinforced thermoplastic polyketone composites. *Composites Part A: Applied Science and Manufacturing*, 126, 105599.
- [6] Eraslan, A. N., & Akis, T. (2006). Transient thermal stresses in composite hollow cylinders subjected to asymmetric temperature fields. *International Journal of Solids and Structures*, 43(10), 3081–3105. <https://doi.org/10.1016/j.ijsolstr.2005.05.045>
- [7] Fairclough, K. A., & Batra, R. C. (2024). Torsion and extension of functionally graded Mooney–Rivlin cylinders. *Journal of Elasticity*, 157(4). <https://doi.org/10.1007/s10659-024-09963-0>
- [8] Hassan, A. H. A., & Kurgan, N. (2022). Modeling functionally graded materials in ANSYS APDL. Research Square. Preprint. <https://doi.org/10.21203/rs.3.rs-1477244/v1>
- [9] Huang, Y., Chen, L., & Zhao, H. (2024). Thermoelastic modeling of functionally graded annular rotating disks under internal and external pressure. *Mechanics of Advanced Materials and Structures*, 31(1), 1–15.
- [10] IzadiGonabadi, H., Oila, A., Yadav, A., et al. (2021). Investigation of anisotropy effects in glass fibre reinforced polymer composites on tensile and shear properties using full-field strain measurement and finite element multiscale techniques. *Journal of Composite Materials*, 56(1), 002199832110542. <https://doi.org/10.1177/002199832110542>

- [11] Liu, Y., Zhang, P., & Qiu, J. (2024). Tension-winding techniques for manufacturing high-performance composite cylinders. *Journal of Reinforced Plastics and Composites*, 43(2), 105–118.
- [12] Mathad, M., Patil, R., Yalagi, S., & Madar, S. (2022). Non-linear structural and thermal analysis of automotive brake disc. *Materials Today: Proceedings*, 59, 1221–1224. <https://doi.org/10.1016/j.matpr.2022.03.426>
- [13] Patel, M. R., & Singh, R. (2019). Review of creep behavior in functionally graded composite cylinders. *Composite Structures*, 223, 110909.
- [14] Rani, P., & Singh, K. (2024). Thermoelastic stress analysis of a functionally graded annular rotating disc with radially varying properties. *International Journal of Engineering Science*, 198, 104052. <https://doi.org/10.1016/j.ijengsci.2023.104052>
- [15] Shahzamanian, M. M., Shahrjerdi, A., Sahari, B. B., & Wu, P. D. (2022). Steady-state thermal analysis of functionally graded rotating disks using finite element and analytical methods. *Materials*, 15, 5548. <https://doi.org/10.3390/ma15155548>
- [16] Sondhi, L., Sahu, R. K., Kumar, R., Yadav, S., Bhowmick, S., & Madan, R. (2024). Functionally graded polar orthotropic rotating disks: Investigating thermoelastic behavior under different boundary conditions. *International Journal on Interactive Design and Manufacturing*, 18(1), 159–166. <https://doi.org/10.1007/s12008-023-01288-7>
- [17] Das, P., Islam, M. A., Somadder, S., & others. (2023). Analytical and numerical solutions of pressurized thickwalled FGM spheres. *Archive of Applied Mechanics*, 93, 2781–2792.
- [18] Wang, L., He, Y., & Sun, F. (2023). Optimization of winding angles for stress control in composite pressure vessels. *Composite Design and Optimization*, 39(3), 215–229.
- [19] Yong, X., Kim, S. J., & Han, Y. (2024). Thermoplastic carbon-fiber sleeves for high-speed permanent magnet motors. *IEEE Transactions on Industrial Electronics*, 71(2), 1881–1892.
- [20] You, J., Lee, Y. M., Choi, H.-H., Kim, T. A., Lee, S.S., & Park, J. H. (2021). Thermally stable and highly recyclable carbon fiber-reinforced polyketone composites based on mechanochemical bond formation. *Composites Part A: Applied Science and Manufacturing*, 142, 106251. <https://doi.org/10.1016/j.compositesa.2020.106251>
- [21] Zhang, X., & Smith, R. J. (2013). Thermo-elastoplastic stress analysis in rotating functionally graded cylinders. *International Journal of Pressure Vessels and Piping*, 110, 1–10.
- [22] Zheng, S., Ding, J., & Zuo, J. (2024). Research on heat dissipation of brake disc in the semi-enclosed space under high-speed train based on fluid-solid-thermal coupling method. *Case Studies in Thermal Engineering*, 56, 104295. <https://doi.org/10.1016/j.csite.2024.104295>
- [23] Timoshenko, S. P., & Goodier, J. N. (1970). *Theory of elasticity* (3rd ed.). McGraw-Hill.
- [24] Zhu, Q., Wang, S., Zhang, D., et al. (2020). Elastoplastic analysis of ultimate bearing capacity for multilayered thick-walled cylinders under internal pressure. *Strength of Materials*, 52(4), 521–531. <https://doi.org/10.1007/s11223-020-00203-9>
- [25] Kumar, R., Sondhi, L., Madan, R., Sahu, R. K., Yadav, S., & Bhowmick, S. (2024, July). Thermo-elastic analysis of functionally graded polar orthotropic rotating disk using collocation method. *Proceedings of the 5th International Structural Integrity Conference & Exhibition (SICE 2024)*.
- [26] Alaghemandi, M., & Alamandi, A. (2025). Heat transfer mechanisms in fiber-reinforced composites: A review. *Thermochimica Acta*, 732, 178905. <https://doi.org/10.1016/j.tca.2025.178905>
- [27] Singh, R., Saxena, R. K., Khanna, K., & Gupta, V. K. (2024). Finite element modeling to analyze creep behavior of functionally graded rotating discs with exponential reinforcement and thickness profiles. *Archive of Applied Mechanics*. Advance online publication. <https://doi.org/10.1007/s00419-024-02626-1>
- [28] Deka, S., Mallick, A., Behera, P. P., & Thamburaja, P. (2020). Thermal stresses in a functionally graded rotating disk: An approximate closed form solution. *Journal of Thermal Stresses*, 44(1), 20–50. <https://doi.org/10.1080/01495739.2020.1843377>
- [29] Okamura, K., Sato, Y., & Takada, S. (2025). Displacement and stress analysis of an elastic hollow disk: Comparison with strength of materials' prediction [Preprint]. arXiv. <https://arxiv.org/abs/2505.03282>

[30] Sato, Y., Ishikawa, H., & Takada, S. (2024). Revisiting stress propagation in a two-dimensional elastic circular disk under diametric loading [Preprint]. arXiv. <https://doi.org/10.48550/arXiv.2401.00126>

[31] Boğa, C., & Yıldırım, V. (2015). Linear elastostatic analysis of functionally graded (FG) rotating disks with hyperbolically varying thickness. XIX National Mechanics Congress, Karadeniz Technical University, Trabzon.

## Nomenclature

All quantities are in SI units. Stresses are reported in **MPa** in figures (1 MPa =  $10^6$  Pa).

Symbol	Description	Unit
$r, \theta, z$	Cylindrical coordinates (radial, circumferential, axial)	m, rad, m
$r_i, r_o$	inner / outer radius	m
$r_0$	Reference radius for material grading	m
$t$	Logarithmic variable in transformation $r = e^t$	-
$u(r)$	Radial displacement	m
$\epsilon_r, \epsilon_\theta, \epsilon_z$	Normal strains (radial, hoop, axial)	
$\sigma_r, \sigma_\theta, \sigma_z$	Normal stresses (radial, hoop, axial)	Mpa
$\tau_{r\theta}$	In-plane shear stress	Pa
$F(r)$	Stress function (problem-dependent)	Pa·m
$E(r)$	Elastic modulus, $E(r)=E_0(r/r_0)^n$	Pa
$E_0$	Reference elastic modulus	Pa
$\rho(r)$	Mass density, $\rho(r)=\rho_0(r/r_0)^\gamma$	kg·m <sup>-3</sup>
$\rho_0$	Reference mass density	kg·m <sup>-3</sup>
$\nu$	Poisson's ratio	-
$n, \gamma$	FGM exponents for $E(r)$ and $\rho(r)$	-
$\omega$	Angular speed	- rad·s <sup>-1</sup>
$\rho(r)\omega^2 r$	Centrifugal body force per unit volume (radial)	N·m <sup>-3</sup>
$R_r, R_\theta$	Distributed body-force components	N·m <sup>-3</sup>
$C_1, C_2$	Integration constants (from boundary conditions)	-
$A$	Particular-solution coefficient	-
$k$	Characteristic parameter from auxiliary equation	-